Emerging magnetic materials for electric vehicle drive motors

Christopher L. Rom,* Rebecca W. Smaha, Shaun O'Donnell, Sita Dugu, and Sage R. Bauers*

Increasing demand for electric vehicles (EVs) is increasing demand for the permanent magnets that drive their motors, as approximately 80% of modern EV drivetrains rely on high-performance permanent magnets to convert electricity into torque. In turn, these high-performance permanent magnets rely on rare earth elements for their magnetic properties. These elements are "critical" (i.e., at risk of limiting the growth of renewable energy technologies such as EVs), which motivates an exploration for alternative materials. In this article, we overview the relevant fundamentals of permanent magnets, describe commercialized and emerging materials, and add perspective on future areas of research. Currently, the leading magnetic material for EV motors is $Nd_2Fe_{14}B$, with samarium-cobalt compounds ($SmCo_5$ and Sm_2Co_{17}) providing the only high-performing commercialized alternative. Emerging materials that address criticality concerns include $Sm_2Fe_{17}N_3$, $Fe_{16}N_2$, and the $L1_0$ structure of FeNi, which use lower cost elements that produce similar magnetic properties. However, these temperature-sensitive materials are incompatible with current metallurgical processing techniques. We provide perspective on how advances in low-temperature synthesis and processing science could unlock new classes of high-performing magnetic materials for a paradigm shift beyond rare earth-based magnets. In doing so, we explore the question: What magnetic materials will drive future EVs?

Introduction

Huge quantities of high-performance permanent magnets (PMs) are needed for continued deployment of renewable energy technologies.[1,2] In particular, the PM motors used in the drivetrains of >80% of electric vehicles (EVs) each require >2 kg of PMs, so massive amounts of PMs will be needed to meet the projected growth in EVs (**Figure 1**).[3] The magnetic materials currently used by these motors contain critical rare earth elements (REEs). While the exact definition of criticality depends on the technoeconomic metrics used, materials are generally considered critical when threats to their supply chain(s) (e.g., geopolitical risks, rising costs, limited availability, etc.) could constrain deployment of the dependent technologies.[3] Many REEs are defined as critical by the US Department of Energy because the dramatic expansion of renewable energy technologies requiring REEs will put increasing pressure on their supply chains. Developing new PM materials can help alleviate this criticality issue. The canonical example of a REE PM is $Nd_2Fe_{14}B$, which was independently discovered and developed in the mid-1980s by researchers in Japan's and the US' automotive industries; it is only fitting that development of next-generation PMs beyond materials such as $Nd_2Fe_{14}B$ is also motivated by mobility.[4,5]

This article focuses on the challenges facing current PM technologies, surveys emerging materials, and adds perspective on future research. We summarize the fundamental physics behind the role of PMs in EV motors, describe the current state-of-the-art as well as the shortcomings therein, and detail some of the emerging technologies at the laboratory and early-startup stage. The authors' background in experimental materials discovery and design inspires our effort to identify how emerging materials hint at broad strategies for discovering and designing new PMs. This discussion is focused on early-stage research of intrinsic materials, though we recognize that for commercialization PMs must be heavily engineered beyond their intrinsic properties. Our overarching goal is to explore the question: What magnetic materials will drive future EV motors?

Christopher L. Rom, Materials Science Center, National Renewable Energy Laboratory, Golden, USA; christopher.rom@nrel.gov
Rebecca W. Smaha, Materials Science Center, National Renewable Energy Laboratory, Golden, USA; rebecca.smaha@nrel.gov
Shaun O'Donnell, Materials Science Center, National Renewable Energy Laboratory, Golden, USA; shaun.odonnell@nrel.gov
Sita Dugu, Materials Science Center, National Renewable Energy Laboratory, Golden, USA; sita.dugu@nrel.gov
Sage R. Bauers, Materials Science Center, National Renewable Energy Laboratory, Golden, USA; sage.bauers@nrel.gov
*Corresponding author
doi:10.1557/s43577-024-00743-4

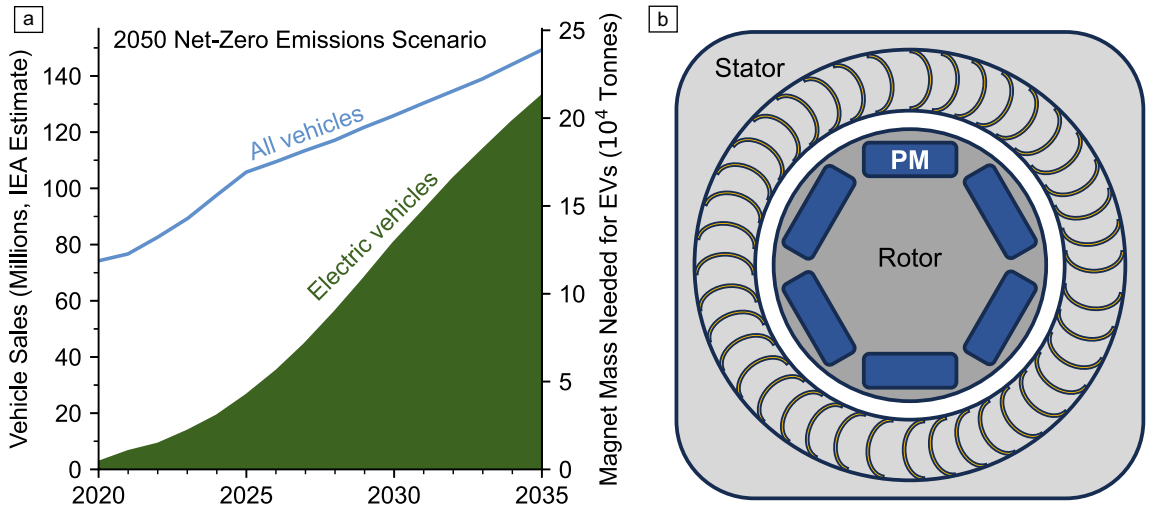

Figure 1. (a) Projected global electric vehicle (EV) sales based on International Energy Agency (IEA) 2050 Net-Zero emissions scenario, adapted from Reference 3. The mass of EV magnets was calculated assuming 2 kg of $Nd_2Fe_{14}B$-based permanent magnets (PMs) per vehicle, with 80% of EVs using PM motors. (b) Schematic representation of an electric drive motor with the PMs radially distributed in the rotor.

Fundamentals of PM motors

(Electro)magnetic repulsion is the basic principle underlying electric drive motors: magnetic fields (B) from a static electromagnet and the PMs repel one another, turning the rotor (Figure 1b). Larger fields therefore lead to more force. PMs enable highly efficient motors because they generate fields without the need for additional energy inputs or moving electrical contacts. A representative magnetic hysteresis loop for a ferromagnetic compound is depicted in **Figure 2**. PM motors operate in quadrant two of this hysteresis loop (Figure 2b) against the opposing magnetic field of the electromagnet (shown as the horizontal axis, H). The PM strength is determined by remanent magnetization M_r, while the coercive field H_c represents its resistance to the opposing field. These terms describe the magnetic energy density $(BH)_{max}$, considered the PM figure of merit, so optimizing them is required for high-performance materials. For a competitive $(BH)_{max}$, it is critical that both M_r and H_c are suitably large. A summary of important terms related to PMs can be found in **Table I**.

How can a phase with intrinsically strong PM parameters—defined in Table I—be identified? Although it is difficult to predict the exact magnetic properties of a phase, there are general chemical trends that can be followed to identify candidates. First, compounds should be rich in open shell 3*d* transition metals (TMs) such as Fe and Ni, which lead to high M_s from the large fraction of unpaired spins. However, TMs alone are often soft ferromagnets, meaning the magnetic moments of each atom align parallel (ferromagnetism), but the net magnetization is easily changed by an opposing field (i.e., soft). To make hard ferromagnets (with large H_c values), magnetocrystalline anisotropy must be induced. Additional nonmagnetic elements (e.g., Al, B, O, N) can cause structural changes that support magnetocrystalline anisotropy, such as cubic to tetragonal distortions. In this case, the goal is to create a uniaxial "easy" crystallographic axis of magnetization, leading to an energy barrier to rotate spins through the concomitant "hard" plane. However, nonmagnetic elements dilute the magnetic atoms reducing M_s and, in anion-rich systems, often lead to ferrimagnetism (e.g., Fe_3O_4) or antiferromagnetism (e.g., Mn_3N_2). The role of REEs in PMs is also to increase magnetocrystalline anisotropy. Through spin–orbit coupling, noninteracting 4*f* electrons align with TM-rich frameworks and lead to high H_c values.

Maintaining a large $(BH)_{max}$ at elevated temperatures is a key design criterion. Even below the ferromagnetic ordering temperature (T_c), performance metrics are influenced by temperature (i.e., softening/weakening as T approaches T_c) as the energy scale of thermal fluctuations becomes comparable to the energy scale of magnetic interactions in a material. Magnets used in EV motors are expected to operate as high as 150–220°C.[8] While the temperature dependence of magnetic properties is strongly affected by microstructural engineering and dopants, identifying a phase's T_C is a functional proxy for most cases. Given that the useful magnetic properties of a phase begin to significantly decrease at ~80% of its T_C, the T_C should be >225°C.[9] In some of the emerging materials discussed below, such as $Fe_{16}N_2$, the material's T_C is higher than its decomposition temperature.[10] Thus, operational thermal stability of the material is an additional key factor that must be considered for practical high-performance magnets.

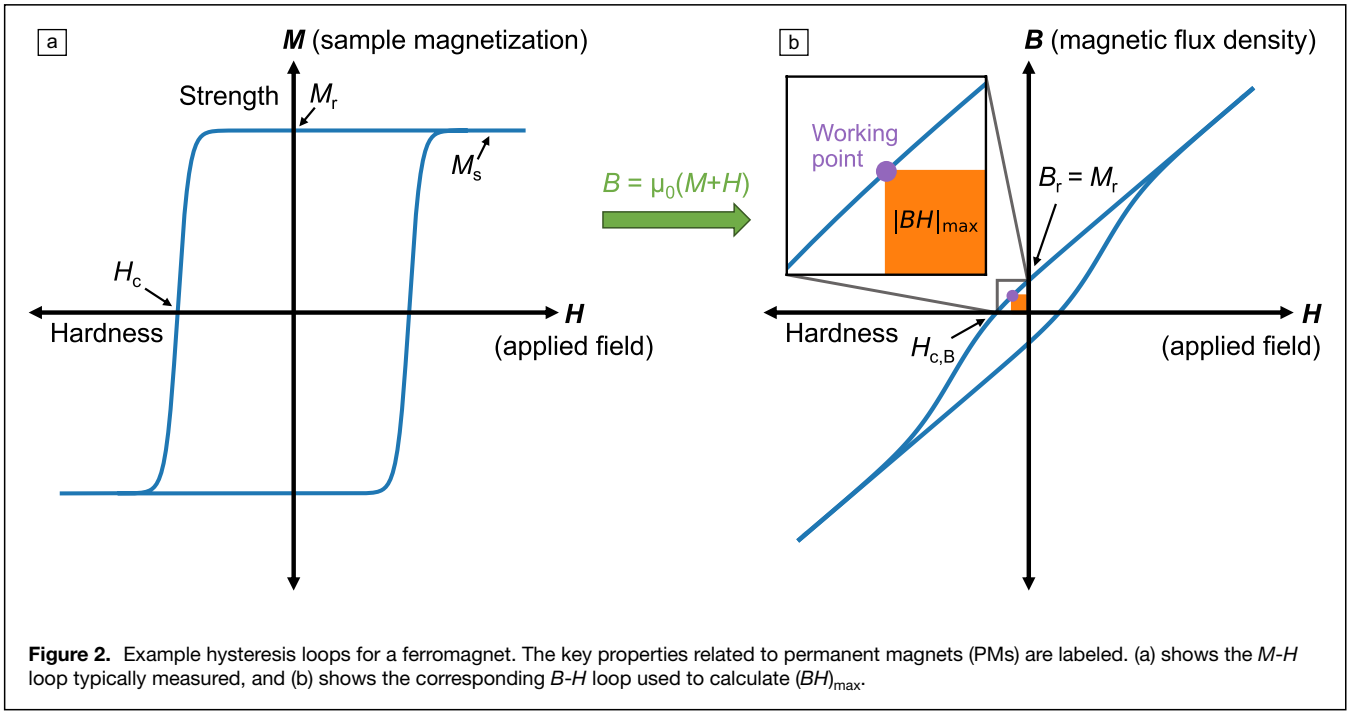

Figure 2. Example hysteresis loops for a ferromagnet. The key properties related to permanent magnets (PMs) are labeled. (a) shows the *M*-*H* loop typically measured, and (b) shows the corresponding *B*-*H* loop used to calculate $(BH)_{max}$.

Table I. Relevant terms for permanent magnets.

• **Magnetic Field** (*H* or *B*): Total field *B* is the sum of the external field (*H*) and the magnetization (*M*) of a material (i.e., $B=\mu_0[H+M]$)
• **Saturation Magnetization** (M_s): Magnetization achieved when all magnetic moments of the ferromagnetic phase are aligned. Units: G or emu/cm^3 (cgs); A·m^2/kg or A/m (SI)
• **Remanent Magnetization** (M_r): Magnetization at zero applied field (same units as M_s). The unitless ratio M_r/M_s is also useful: ideally as close to 1 as possible
• **Coercivity** (H_c): Value of the applied opposing field needed to reduce *M* to zero (i.e., demagnetize the sample). Arises from a combination of intrinsic (material property) and extrinsic (microstructure property) magnetic anisotropy. Units: Oe (cgs); T or A/m (SI)
• **Magnetocrystalline Anisotropy**: An intrinsic property related to the anisotropy field (H_a) needed to rotate a domain between crystallographic axes. Units: Oe (cgs); T or A/m (SI)
• **Magnetic Energy Density** ($(BH)_{max}$): The maximum magnetostatic energy of a PM. Measured as the maximal product of $\lvert B{\cdot}H\rvert$ on demagnetization. Units: MGOe (cgs); kJ/m^3 (SI)
• **Curie Temperature** (T_C): Temperature below which the atomic magnetic moments of the ferromagnetic phase are ordered. Above this temperature, there is no net magnetization
• **Temperature Coefficient**: As key magnetic terms tend to decrease with increasing temperature, the rate of decrease is often quantified in a derivative (e.g., dH_c/dT). Units: %/K

These values can be determined via magnetic susceptibility measurements as detailed by Reference 6. Magnetic units are notoriously confusing, as CGS and SI standards are both in active use.[7]

Currently commercialized PM materials

The highest-performing commercialized magnets contain REEs: Sm-Co and Nd-Fe-B magnets. As previously described, REEs improve key properties of ferromagnets. Next, we distill a few lessons from these examples.

Samarium-cobalt magnets

Sm-Co magnets were developed in the early 1950s and were among the first materials with large enough H_c to resist reorienting against a reverse field. This meant a useful torque could be generated, spurring interest in PM motors.[11] There are two main stoichiometries with good PM properties: $SmCo_5$ and Sm_2Co_{17}. These phases share high T_C and very large H_c—the greatest of any commercialized magnet. $SmCo_5$ (**Figure 3**a) possesses a giant axial magnetocrystalline anisotropy resulting from the unquenched prolate *f*-electron density of Sm ions, with orbital moments aligned parallel to spin moments of Co (Figure 3d).[12,13] The Sm *f* shell aligns along the crystallographic *c*-axis, because this minimizes Coulombic interaction with the crystal field of hexagonal Co layers, and strong spin–orbit coupling concomitantly aligns spins.[14] $SmCo_5$ is hexagonal; however, Sm_2Co_{17} is either hexagonal or rhombohedral depending on the stacking sequence of the mixed Sm-Co planes (Figure 3b–c). The magnetocrystalline

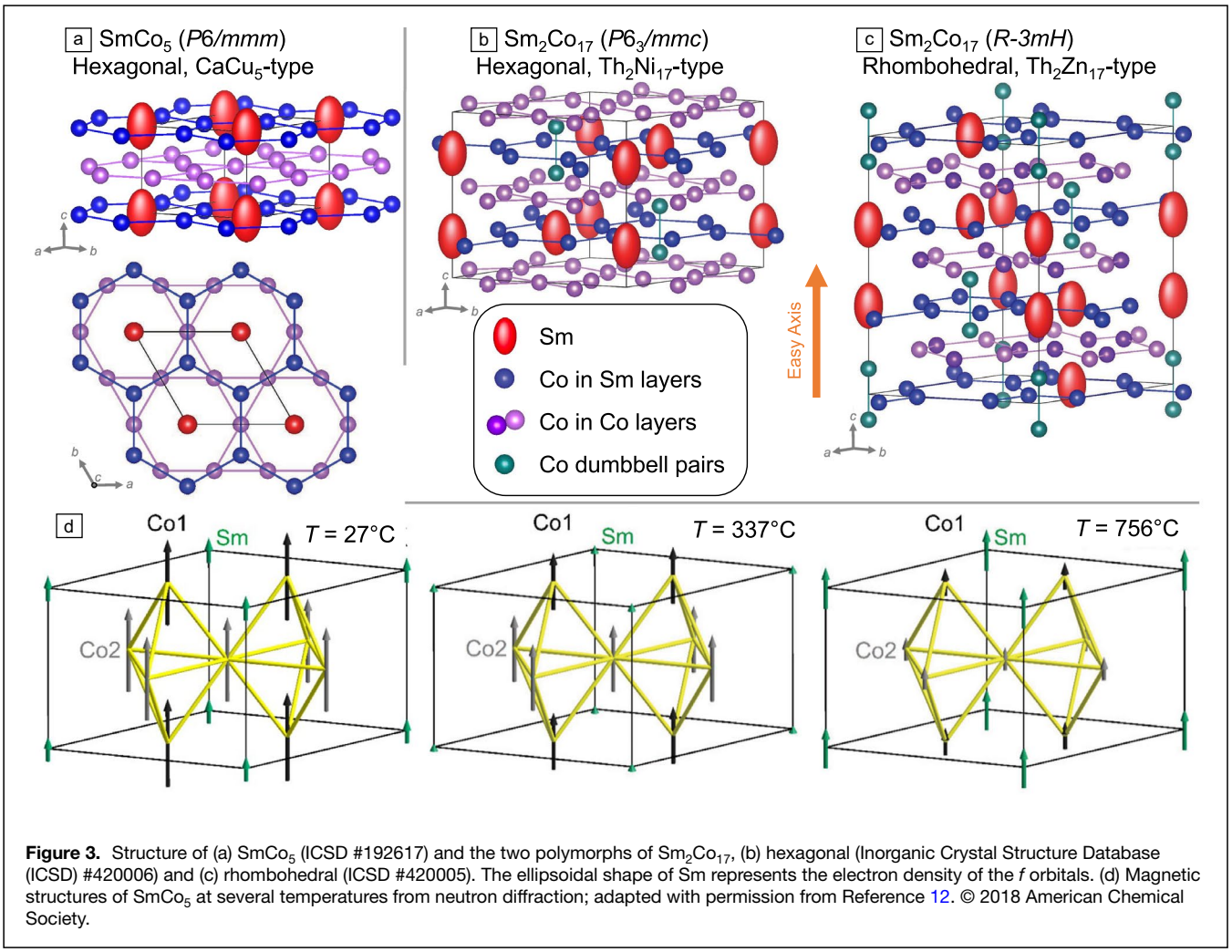

Figure 3. Structure of (a) $SmCo_5$ (ICSD #192617) and the two polymorphs of Sm_2Co_{17}, (b) hexagonal (Inorganic Crystal Structure Database (ICSD) #420006) and (c) rhombohedral (ICSD #420005). The ellipsoidal shape of Sm represents the electron density of the *f* orbitals. (d) Magnetic structures of $SmCo_5$ at several temperatures from neutron diffraction; adapted with permission from Reference 12. © 2018 American Chemical Society.

anisotropy of Sm_2Co_{17} is one-fourth that of $SmCo_5$ because the Co–Co dumbbells that replace some of the Sm lead to multiple easy magnetization directions, reducing overall anisotropy.[15] Although Sm-Co magnets played an important role in the development of PM electric motors, they suffer from lower magnetization and higher cost than competitors, making them only appropriate for niche applications, especially those requiring high temperatures.

Neodymium iron boride ($Nd_2Fe_{14}B$)

The discovery of REE-based PM neodymium iron boride ($Nd_2Fe_{14}B$) ushered in an exciting new era in PM research. $Nd_2Fe_{14}B$ has a tetragonal structure with strong uniaxial anisotropy: the *c*-axis is its easy axis of magnetization (**Figure 4**). Each B is coordinated by six Fe in a distorted trigonal prismatic environment. Two of the B-occupied prisms share an edge, creating quasi-0D $Fe_{10}B_2$ "bowties" punctuating a matrix otherwise comprising Fe and Nd. The large fraction of Fe contributes a large M_s (38 μ_B per formula unit), and the tetragonality induced by B (alongside magnetocrystalline anisotropy from Nd *f* orbitals) leads to an anisotropy field ($\mu_o H_a$) of 6.7 T at room temperature.[16] This high performance has led $Nd_2Fe_{14}B$ to be the primary magnet material for EV motors.[3]

Though $Nd_2Fe_{14}B$ has a high $(BH)_{max}$ at room temperature, its performance declines dramatically with increasing temperature (**Figure 5**a). To meet the elevated temperature conditions in EV motors, heavy REEs such as Dy or Tb are partially substituted for Nd to form $(Nd,Dy/Tb)_2Fe_{14}B$, which increases the magnetocrystalline anisotropy and T_C, resulting in higher coercivity and better thermal performance.[17,18] However, incorporation of Dy deteriorates the magnetization as both the orbital and spin magnetic moments of the heavy REEs couple antiferromagnetically with those of Fe in $(Nd,Dy)Fe_{14}B$. Significant effort has been applied to engineer the microstructure of $Nd_2Fe_{14}B$ magnets in hopes of reducing or eliminating reliance on Dy, but heavy REEs—which are generally considered more critical—remain the most effective way to maintain the $(BH)_{max}$ of $Nd_2Fe_{14}B$ at elevated temperatures.[19–21] The temperature dependence of $(BH)_{max}$ values of these established materials are shown in Figure 5a.

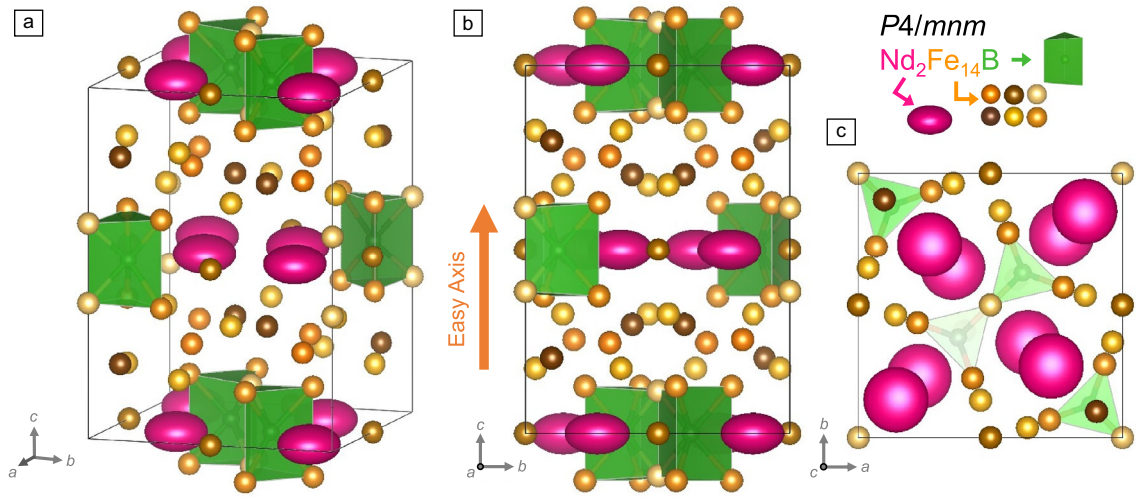

Figure 4. The crystal structure of $Nd_2Fe_{14}B$ (ICSD #48143) viewed (a) from a tilted perspective, (b) down the *a*-axis, and (c) down the *c*-axis. The oblate shape of Nd represents the electron density distribution of the *f* orbitals.[13]

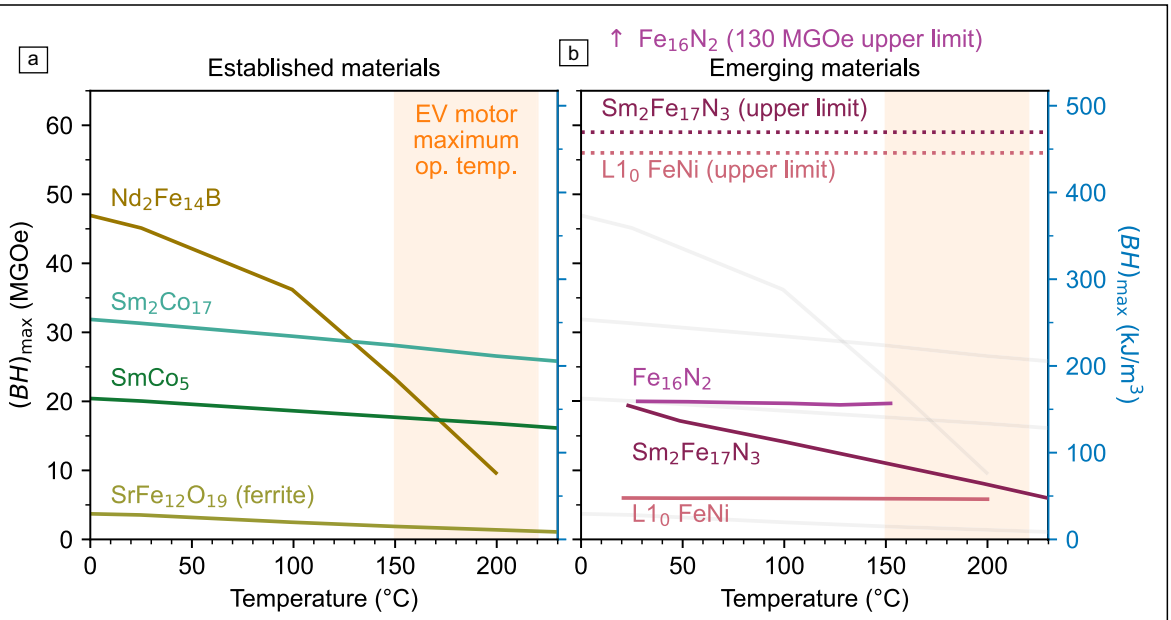

Figure 5. Temperature dependence of $(BH)_{max}$ for (a) established permanent magnet (PM) materials compared with (b) emerging PM materials. Values were extracted from References 10, 22, 24–26, 37. The temperature dependences of emerging materials were estimated using reported temperature dependences of B_r and H_c. The theoretical upper limits are from Reference 22, with the limit for $Fe_{16}N_2$ off the chart. The maximum operating temperature region for electric vehicle motors is highlighted in orange. The *y*-axis range and scale are the same in both panes with left and right axes representing different units.

Other commercialized magnets

Many other magnetic materials have been researched, and several have been commercialized, but they are too weak or expensive for EV applications. Ferrite-based magnets (e.g., $SrFe_{12}O_{19}$) are low-cost and widespread but weak ($(BH)_{max} \sim 5$ MGOe).[22] Alnico magnets (composite alloys of Fe with Al, Ni, and Co) are moderately powerful ($(BH)_{max} \sim 10$ MGOe) but tend to be high-cost relative to their performance.[9,22] Although analysis based on electron microscopy suggests that optimizing the microstructure of Alnico could improve $(BH)_{max}$ to ~20 MGOe,[23] this upper limit still falls below the performance of REE magnets.

Criticality issues

Resource challenges limit the scalability of current high-performance REE magnets. These challenges include high costs associated with scarce and difficult-to-refine elements, supply chain risks, or both. As shown in **Figure 6**, REEs are not the only materials constrained by these challenges: Co too suffers as it is the most expensive 3*d* metal and is heavily used by other EV technologies, such as batteries. These

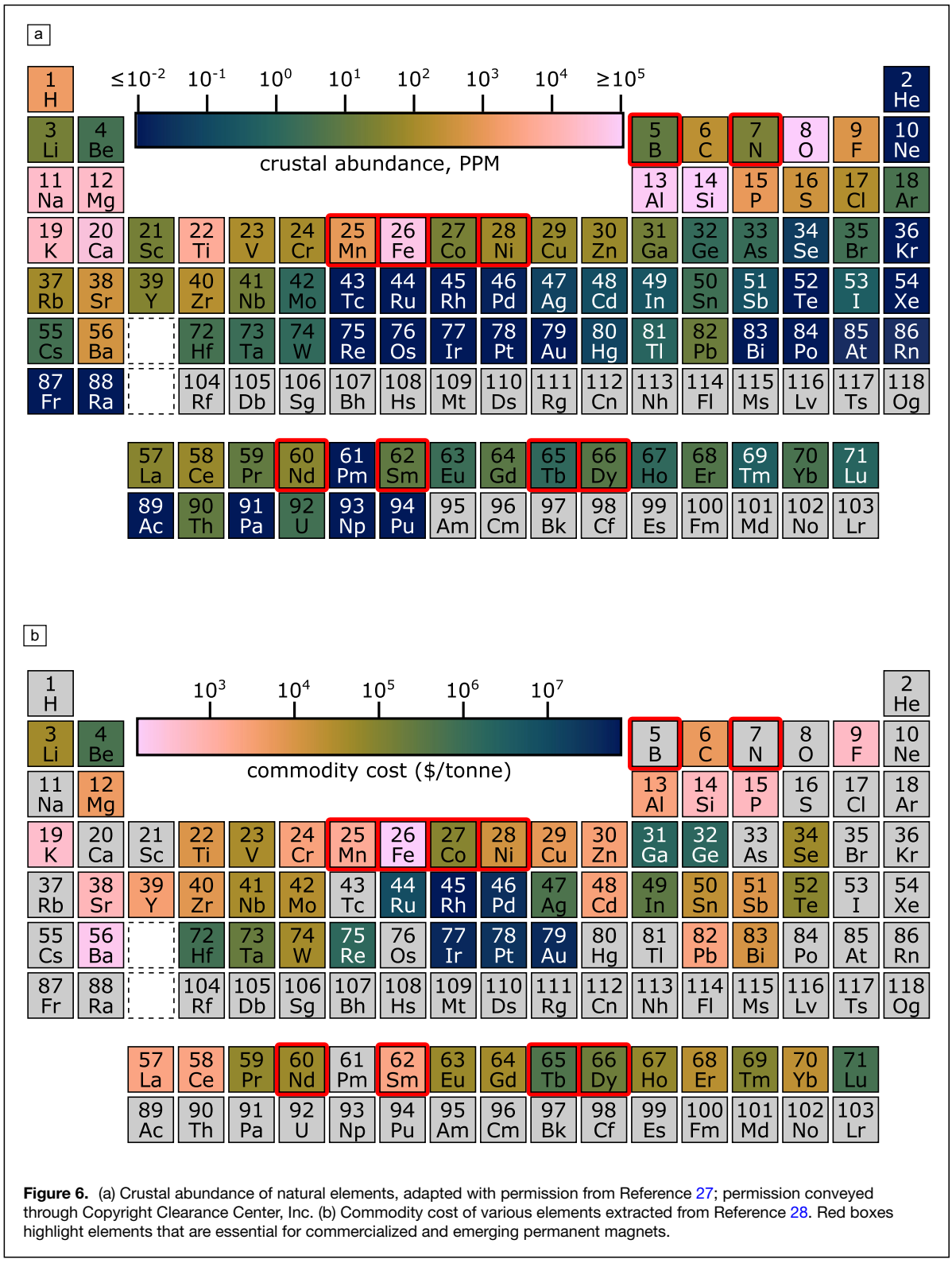

Figure 6. (a) Crustal abundance of natural elements, adapted with permission from Reference 27; permission conveyed through Copyright Clearance Center, Inc. (b) Commodity cost of various elements extracted from Reference 28. Red boxes highlight elements that are essential for commercialized and emerging permanent magnets.

criticality issues could hinder the deployment of technologies based on the current high-performing magnets ($Nd_2Fe_{14}B$ and Co-Sm).

What elements should applications-focused researchers prioritize? Ideally, the elements should be low-cost, low-toxicity, produced in large quantities, and support large $(BH)_{max}$. Fe tops the list. Mn could also supply large magnetic moments with low materials costs. As 4*d* and 5*d* metals could boost coercivity via spin–orbit coupling, Zr, Nb, Mo, and W could also be important constituents of future low-cost high-performance magnets. Sm is a low-cost REE, as there are currently no large-scale applications of the element. However, criticality could change over time with market conditions and technological development. Research using critical elements can reveal valuable fundamental insights, but researchers should be clear-eyed about scalability, economic, and social (as well as technical) challenges.

Emerging PM materials

Three emerging materials show the greatest promise for near-term development as magnets for EVs: $Sm_2Fe_{17}N_3$, $Fe_{16}N_2$, and the $L1_0$ structure of FeNi. These materials exhibit both promising magnetic properties (Figure 5b) and comprise (relatively) low-cost elements. However, these phases are less thermally stable than established technologies, so new processing techniques will be needed to realize their potential.

$Sm_2Fe_{17}N_3$

One path to reduce criticality concerns is via REE-based materials that contain either a lower REE fraction and/or REE elements that are less critical than Nd and Dy. Building off the exceptional magnetic properties of $SmCo_5$ and Sm_2Co_{17}, other materials in these and related families were investigated beginning in the 1980s. To mitigate the use of Co, Fe-rich intermetallics in structure types such as $ThMn_{12}$ (e.g., $REFe_{11}Ti$), Th_2Zn_{17}, Th_2Ni_{17}, and $CaCu_5$ were studied.[29,30] However, their magnetic properties were often lacking in some important aspect, generally with low Curie temperatures and limited saturation magnetizations. For example, the RE_2Fe_{17} series has T_Cs that are approximately 700–800°C lower than the analogous RE_2Co_{17} series.[30]

One strategy to circumvent these challenges is through intercalation. A breakthrough came in 1990, with the discovery that N intercalation into RE_2Fe_{17} increases the unit-cell volume by 6–7% and thus greatly improves its magnetic properties by strengthening Fe–Fe interactions (**Figure 7**).[31] The T_C of Sm_2Fe_{17} increases from approximately 120 to 480°C; the M_s increases by 50% despite a lower magnetic ion fraction; and the magnetocrystalline anisotropy increases with a N content of approximately $Sm_2Fe_{17}N_{2.7}$.[32,33] While other intercalants like C and H similarly expand the lattice and improve properties,[31,34,35] N produces the greatest expansion and improvement, with an intercalation level of $Sm_2Fe_{17}N_3$ yielding the optimal magnetic properties.[36] Moreover, while Sm is a REE, its relative abundance, co-location with other REEs in ores, and lack of other technological uses lead to currently low commodity costs (cf. Figure 6). This sparked a flurry of research into $Sm_2Fe_{17}N_3$ that continues to the present.[37] However, the major challenge facing $Sm_2Fe_{17}N_3$ is thermal stability: $Sm_2Fe_{17}N_3$ begins losing N at 600°C under N_2 atmosphere and 200°C under vacuum,[38] so while the material should be operationally stable in a drive motor, development of low-temperature densification methods is necessary before sintered PMs can be fabricated.

$Fe_{16}N_2$

A leading contender for REE-free PMs for EVs is α''-$Fe_{16}N_2$ (referred to here as $Fe_{16}N_2$). It exhibits an

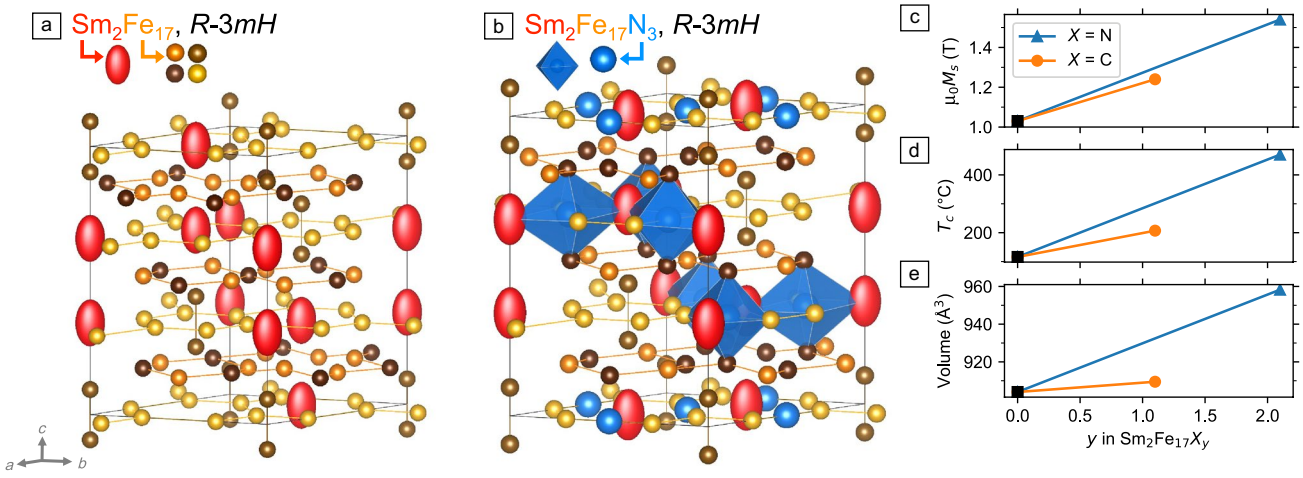

Figure 7. Crystal structures of (a) Sm_2Fe_{17} (ICSD #96064) and (b) $Sm_2Fe_{17}N_3$ (ICSD #192366). Sm is shown as ellipsoids to indicate *f* orbital polarity; Intercalation of N or C into Sm_2Fe_{17} boosts (c) magnetization, (d) increases T_C, and (e) expands the lattice volume. (c–e) Adapted with permission from Reference 31. © 1990 Elsevier.

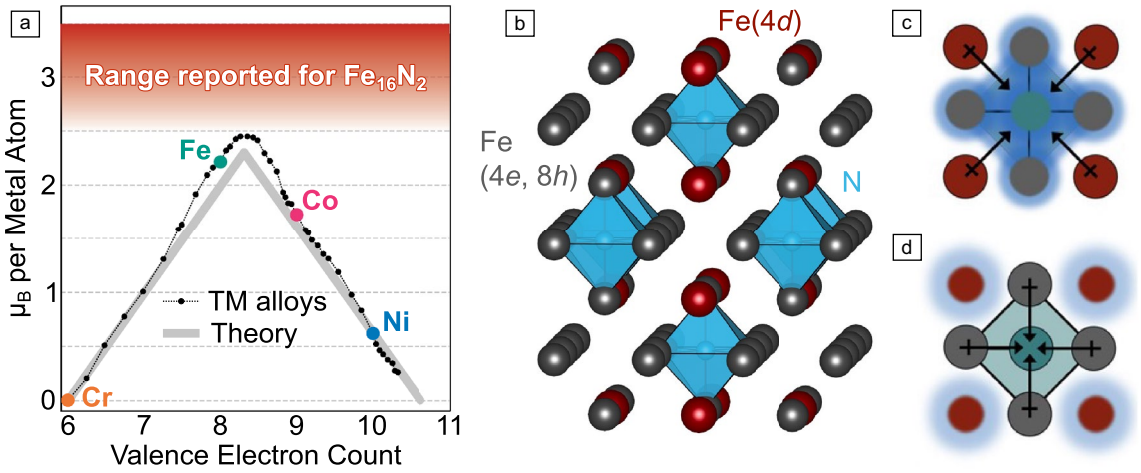

Figure 8. (a) Slater–Pauling curve for the magnetic moment of transition-metal alloys compared to the magnetic moments reported for $Fe_{16}N_2$; extracted from References 39, 47. (b) $Fe_{16}N_2$ structure schematic with Fe Wyckoff positions labeled. (c, d) Magnetic structure hypotheses for $Fe_{16}N_2$: (c) Hypothesis I – anionic clusters from Fe–N bonding leads to oxidation and increased moment of the Fe-4*d* atoms versus (d) Hypothesis II – oxidation of Fe bound to N yields a higher local moment on the Fe-4*e*, 8*h* atoms embedded in an Fe^0 matrix. Electron-rich Fe species are shaded blue.

extremely high M_s of 2200 emu/cm^3, which leads to a theoretical maximum $(BH)_{max}$ of $\mu_0 M_s^2/4 \approx 130$ MGOe.[39] To date, the highest $(BH)_{max}$ reported for $Fe_{16}N_2$ is 20 MGOe, where this energy density is primarily limited by low H_c.[10,40] Notably, $Fe_{16}N_2$ exhibits an excellent temperature coefficient with $(BH)_{max}$ decreasing only slightly at elevated temperature (Figure 5b). Given its moderate magnetocrystalline anisotropy (1.8 MJ/m^3), improvements to H_c should be possible. Importantly, $Fe_{16}N_2$ faces no criticality challenges: Fe and N rank 1st and 3rd on the list of highest-volume global chemical production.[41] $Fe_{16}N_2$ is currently undergoing commercialization.[42]

Although the large M_s of $Fe_{16}N_2$ was initially discovered in the 1970s,[43] the slow development of this material stems from the difficulty of synthesizing it.[39] $Fe_{16}N_2$ is deeply metastable and decomposes above 200°C, well below its estimated T_C (~380°C).[10] Additionally, achieving the necessary order on the N sublattice, which is required to realize the materials properties noted above, has proved exceedingly difficult. Synthetic approaches often rely on out-of-equilibrium processes to kinetically trap N in the solid, followed by low-temperature annealing to induce anion ordering.[40,44,45] $Fe_{16}N_2$ can be made as both thin films and bulk powders.[39]

The powerful magnetism of $Fe_{16}N_2$ comes from its unique structure. The range of M_s in literature far exceeds the value predicted by the Slater–Pauling curve, which relates the electron count of TM alloys to their magnetic moment (**Figure 8**a). $Fe_{16}N_2$ adopts a tetragonal structure that can be described as Fe_8N with the interstitial, octahedrally coordinated N atoms in the body-centered-tetragonal (bct) Fe lattice arranged into an ordered supercell (Figure 8b). This leads to an overarching structural motif of quasi-0D anion-metal polyhedra dispersed throughout a metal matrix. This motif can also be described as a partial N interstitial in a Cu_3Au structure, which has recently been shown to yield high magnetic performance in Ni_3MnN and Mn_3IrN.[46]

The magnetic structure of $Fe_{16}N_2$ is still under active debate. Two polarized neutron studies have concluded different models: an earlier study[48] concluded that crystallographic site Fe-4*d* (Figure 8b) has the largest moment, while a later study[49] concluded that site Fe-8*h* has the highest moment. Both measurements were plagued by experimental uncertainty, yet despite their disagreement, both reports concluded that there is a fundamental difference between Fe atoms bound in the [NFe_6] cluster compared to Fe atoms outside the cluster. These discrepancies give rise to two contrasting possible mechanisms for the physics of $Fe_{16}N_2$, shown in Figure 8c–d. In one hypothesis, the N pulls electron density into the Fe of the octahedral cluster (Figure 8c); in the other, the N-centered octahedra push electron density out to the Fe-4*d* site (Figure 8d).

$L1_0$ FeNi

The mineral tetrataenite, also known as $L1_0$ FeNi, is another REE-free PM contender, albeit less developed than $Sm_2Fe_{17}N_3$ or $Fe_{16}N_2$. "$L1_0$" denotes the CuAu structure type. $L1_0$ FeNi exhibits magnetic hardness that arises from the ordering of the metals into alternating sheets (**Figure 9**). In their disordered alloy, Fe and Ni randomly occupy sites on a face-centered-cubic (fcc) lattice (*Fm*-3*m*), resulting in a soft magnet. For the magnetically hard $L1_0$ structure, Fe and Ni layers alternate

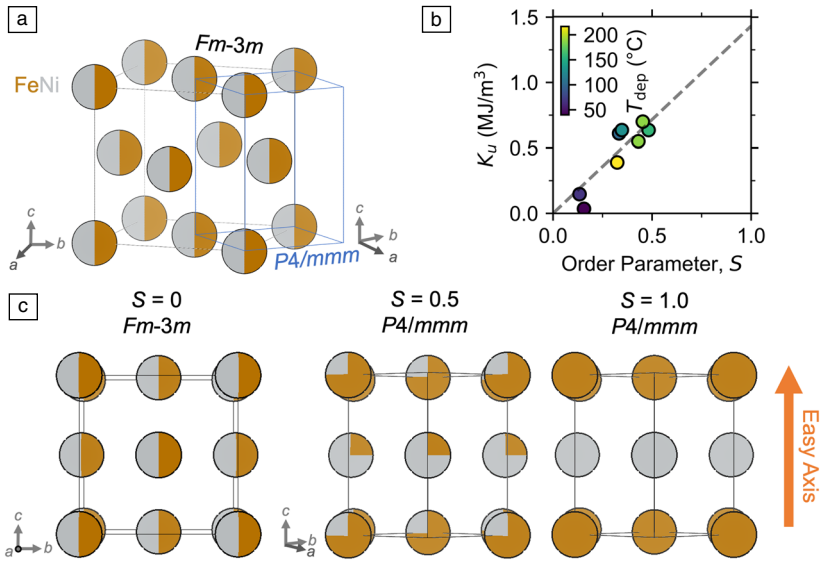

Figure 9. (a) The $L1_0$ structure of FeNi is an ordered tetragonal (*P4/mmm*) variation of the disordered cubic (*Fm-3m*) FeNi alloy. (b) Experimental correlation of order parameter *S* (describing the degree of Fe–Ni ordering) with the magnetocrystalline anisotropy constant K_u. The dashed gray line is a linear fit to the data. Adapted with permission from Reference 51. (c) Depiction of FeNi polytypes: disordered (*Fm-3m*), partially ordered, and fully ordered ($L1_0$, *P4/mmm*).

along fcc (001), creating a concomitant tetragonal distortion (*P4/mmm*). The degree of metal ordering/tetragonality can be quantified via an order parameter *S,* where $S=1$ indicates fully ordered $L1_0$ FeNi and $S=0$ indicates fully disordered FeNi.[50] Experiments on thin films demonstrate that the anisotropy constant (K_u) is proportional to *S*, as shown in Figure 9b.[51] Thin-film experiments have achieved ordering as high as $S=0.48$,[51] while bulk methods reached $S=0.71$.[50] The naturally occurring tetrataenite found in meteorites likely has *S* near 0.5–0.6 based on magnetic anisotropy measurements[52] and Mossbauer spectroscopy.[53]

Unfortunately, $L1_0$ FeNi is difficult to realize in the laboratory with high purity because solid-state diffusion is slow around the ordering temperature (ca. 320°C). The prevailing hypothesis for the natural formation of tetrataenite is that the astronomical timescales afforded by deep space asteroids with slow cooling rates (1–5°C per million years) allowed the atoms enough time to slowly diffuse into the ordered, thermodynamically stable $L1_0$ FeNi phase.[54] On Earth, the initial discovery of $L1_0$ FeNi used neutron bombardment to enhance diffusion near 320°C.[55,56] Recently, the simultaneous application of stress and an external magnetic field has shown promise for inducing order.[53]

Although $L1_0$ FeNi has not yet been fabricated into PMs, the material should withstand the operating temperatures of drive motors. The magnetic properties of $L1_0$ FeNi exhibit only small decreases with increasing temperature (Figure 5b).[25] And while the thermodynamic order–disorder transition is ~320°C,[56] differential scanning calorimetry shows tetrataenite is kinetically trapped up to 530°C.[57] These values are well above the maximum temperatures reached by EV drive motors (ca. 150–220°C). However, as with $Sm_2Fe_{17}N_3$ and $Fe_{16}N_2$, synthesis and processing remain a challenge, as will be discussed in the "Perspective" section.

Other emerging magnetic materials

Although there are numerous other emerging magnetic materials of great scientific interest, none are poised for incorporation into EVs soon. Other magnetic materials with the lowest supply risk (e.g., MnAl- and MnBi-based magnets) are about as powerful as Alnico magnets ($(BH)_{max}$ ~ 10 MGOe),[22,58] so seem unlikely to replace the current REE-based magnets in drive motor applications. Although more powerful magnets are found in this class of newer REE-free materials (e.g., Zr_2Co_{11}, $HfCo_5$, Co_3Si) with $(BH)_{max}$ values on the order of 10–20 MGOe,[22,59,60] these materials face criticality challenges owing to their use of Co (or Hf).[3] Additionally, there are many other materials that are not suitable for PM applications themselves (owing to low overall magnetization) but which demonstrate design principles that may be useful for guiding further materials discovery efforts (e.g., $Hf_2FeIr_5B_2$, $Li_2(Li_{1-x}Fe_x)N$, and $MnBi_2$). The ultimate goal is to match or exceed the performance of REE magnets with lower cost and less supply-constrained elements.

Perspective

Design philosophy for disruptive magnetic materials

The emerging magnetic materials discussed in this article have been known for many decades. Next, we explore what limits these materials from commercialization and provide perspective on challenges for new magnetic materials discovery.

Why have these emerging materials not yet been functionalized into commercially viable magnets?

Current commercialized high-performance PM materials rely on metallurgical processing techniques, which do not necessarily apply to these emerging materials. For example, the processing for $Nd_2Fe_{14}B$ includes strategies such as rapidly quenching from melt, milling to control dispersion,

and sintering to make fully dense magnets.[9] In contrast, the most promising emerging materials previously discussed—$Sm_2Fe_{17}N_3$, $Fe_{16}N_2$, and $L1_0$ FeNi—require gentler processing, and the challenges to each are unique. While $Sm_2Fe_{17}N_3$ is stable at ambient conditions, it becomes metastable against N_2 loss at about 600°C, thus requiring altogether new sintering approaches to densify. Similarly, $L1_0$ FeNi is stable at ambient temperatures, but is impossible to make via metallurgical approaches because high-temperature processing results in Fe–Ni disorder. $Fe_{16}N_2$ has both synthetic challenges (i.e., N_2 effusion and N vacancy order/disorder) but is made more difficult still due to its ambient condition metastability. And once synthesized, the stability of the material must be maintained in the operating environment of the PM (i.e., protected from air and excessive heat under drive-motor conditions). Novel "beyond metallurgy" techniques are being rapidly developed to overcome these challenges; eventually, they may be extended to other potential PM materials that have been historically underexplored due to their metastability and/or volatile anion chemistry.

What chemical and physical features can we extract from the emerging magnetic materials, or other observations of desirable magnetic properties, to instill into new materials?

It is curious that two of the most promising magnetic materials are dilute nitrides given that the most common PM, $Nd_2Fe_{14}B$, contains dilute B. However, perhaps this is not surprising: Fe has a $>d^5$ electron configuration, so the introduction of a more electronegative anion can reasonably increase the unpaired electron density on Fe (cf. Figure 8). Relative to boron, stronger/more polarizing anions like nitrogen could also enable larger distortions from high-symmetry structures, providing an avenue to design uniaxial symmetry. On the other hand, too strong an anion leads to anion-rich materials with superexchange-mediated antiferromagnetic or ferrimagnetic configurations, as seen in ferrites. Convoluted with this electronic effect, anionic N is also larger than anionic B and C, increasing the unit-cell volume and improving magnetic properties, as observed in $Sm_2Fe_{17}N_3$. Thus, the observation that many emerging PMs are subnitrides might not be a coincidence at all—N could represent an ideal anion to promote ferromagnetism, motivating the discovery of new nitrides and materials with similar anion electronegativity (e.g., C, P, S, Cl, Br).

How can we predict, in an efficient way, new materials that will have high magnetic performance?

Although several informatics-based papers have been published on the identification of potential PM materials,[61–63] the vast majority take the approach of down-selecting known phases. While there is some work on decorating known lattices with various chemical substitutions to predict new materials,[64] we are unaware of any works that extend the breadth of the search into new chemistries and structural prototypes in a generalized, high-throughput way. While such approaches are rapidly being developed to predict the existence of new/unknown anion-rich phases,[65] their underlying algorithms are based on ionic substitution so are likely unsuitable for PM candidates without formal ionic bonding. Thus, an open challenge to the materials informatics community is establishing a means to predict the stability, structure, and magnetic properties of *new* materials. In the absence of high-throughput computational frameworks, we posit a few design features based on our observations of emerging materials.

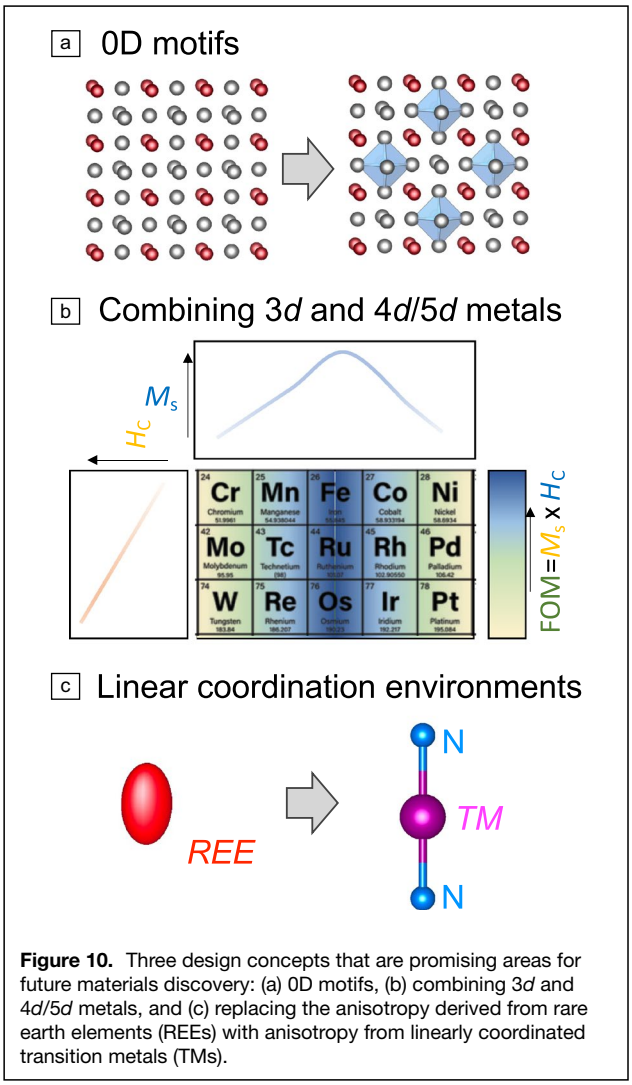

Figure 10. Three design concepts that are promising areas for future materials discovery: (a) 0D motifs, (b) combining 3*d* and 4*d*/5*d* metals, and (c) replacing the anisotropy derived from rare earth elements (REEs) with anisotropy from linearly coordinated transition metals (TMs).

Identifying compelling features for next-generation magnetic materials

We identify three design features we believe will be important for discovering new magnetic materials for high-performance PM applications (**Figure 10**). These features are: (a) 0D materials with isolated anion-centered polyhedra (inspired by $Nd_2Fe_{14}B$, $Fe_{16}N_2$, and $Sm_2Fe_{17}N_3$); (b) combining 3*d* elements (for high

M_s) with 4*d* and 5*d* elements (for high H_c from spin–orbit coupling); and (c) linear coordination environments for 3*d* metals. Our review of the literature suggests these features are underexplored and may yield powerful new PM materials.

First, 0D structural elements in $Nd_2Fe_{14}B$ (B-centered bowties) and $Fe_{16}N_2$ (N-centered octahedra) suggest that 0D anion-centered polyhedra may be an intriguing design feature. As described previously, neutron diffraction studies on $Fe_{16}N_2$ present conflicting arguments for how the ordered N affect the charge distribution (and thus, the magnetism) compared to bcc Fe. Although the exact cause is uncertain, the result is strong ferromagnetism. A similar enhancement of M_s is seen in the conversion of Sm_2Fe_{17} to $Sm_2Fe_{17}N_3$. Future exploration of compounds with dilute anions may resolve this uncertainty. In doing so, new materials with quasi-0D motifs may be revealed to have powerful magnetism.

Second, the combination of 3*d* with 5*d* (or 4*d*) transition metals is a well-worn strategy for PM materials discovery, yet the space has not been explored comprehensively. Here, high M_s can come from 3*d* metals, and high spin–orbit coupling from 4*d* or 5*d* metals (which leads to high magnetocrystalline anisotropy and high H_c). MnBi, $HfCo_7$, and Zr_2Co_{11} are well-developed examples of this concept.[58,60] The recent discovery of $MnBi_2$ suggests there is further room for exploration in even simple binary phase spaces.[66] Work on multinary systems such as $Hf_2MIr_5B_2$ (M=Mn, Fe) experimentally demonstrates the boost to magnetic anisotropy from heavy elements.[67] There are an enormous number of possible elemental combinations and structural configurations in this space, with a great deal yet to be explored. One area that appears ripe for systematic study is connecting the bond character of these systems to magnetic properties.

Finally, linear coordination environments may also enhance H_c via spin–orbit coupling. $Li_{3x}Fe_xN$ highlights the impact of this structural feature on magnetic properties. Although too Fe-poor for PM applications, the linearly coordinated Fe exhibit high saturation magnetic moments ($\mu^{\|} \sim 5\mu_B$) and giant magnetocrystalline anisotropy with $\mu_0 H_c = 11.6$ T.[68] This arises because the linear coordination environment preserves spin–orbit coupling, which is otherwise quenched in 3*d* metals. Linearly coordinated motifs cannot undergo first-order Jahn–Teller distortions, which preserves the orbital angular momentum. Similar behavior is observed in organometallic compounds with linearly coordinated Fe.[69] $Li_{3-x}Fe_xN$ in essence behaves as a collection of highly anisotropic single-ion magnets. Finding such geometries in phases with higher 3*d* metal density is an extremely promising path toward high performance REE-free PMs.

Summary and outlook

The accelerating demand for EVs is increasing the need for new PM materials. Current magnet technologies are heavily dependent on metals with critical supply risks (e.g., Nd, Dy, Co). Scaling up the production of PM-based electric motors will require the development of new materials; $Sm_2Fe_{17}N_3$, $Fe_{16}N_2$, and $L1_0$ FeNi are the current most promising candidates. These emerging materials exhibit high magnetic energy densities with the potential to compete with established technologies and are composed of less critical materials. Advances in materials processing beyond traditional metallurgical methods are needed to boost the coercivity of these emerging materials. Beyond these three candidates, we hypothesize that materials discovery efforts could further realize promising new magnetic materials. We propose several design concepts toward this goal: 0D motifs, combining 3*d* with 4*d*/5*d* transition metals, and using linearly coordinated transition metals to replace the magnetic anisotropy currently provided by rare earth elements. The need to develop and scale up new magnetic materials is urgent, but the opportunity for new discoveries is similarly great.

Acknowledgments

This work was authored by the National Renewable Energy Laboratory, operated by Alliance for Sustainable Energy, LLC, for the US Department of Energy (DOE) under Contract No. DE-AC36-08GO28308. Funding provided by the US Department of Energy, Office of Science, Basic Energy Sciences, Division of Materials Science, through the Office of Science Funding Opportunity Announcement (FOA) No. DE-FOA-0002676: Chemical and Materials Sciences to Advance Clean-Energy Technologies and Transform Manufacturing. The views expressed in the article do not necessarily represent the views of the DOE or the US Government. The authors thank their wonderful collaborators J. Neilson, A. Zakutayev, and W. Sun for countless valuable conversations and providing inspiration for Figures 8c, d, and 10b.

Author contributions

Conceptualization: C.L.R. and S.R.B.; visualization: C.L.R. and S.R.B.; supervision: S.R.B.; writing–original draft: C.L.R., R.W.S., S.O., S.D., and S.R.B.; writing–review and editing: C.L.R., R.W.S., S.O., S.D., and S.R.B.

Funding

Open access funding provided by National Renewable Energy Laboratory Library. Funding provided by the US Department of Energy, Office of Science, Basic Energy Sciences, Division of Materials Science, through the Office of Science Funding Opportunity Announcement (FOA) No. DE-FOA-0002676: Chemical and Materials Sciences to Advance Clean-Energy Technologies and Transform Manufacturing.

Data availability

No new data were generated for this article.

Conflict of interest

Several of the authors (Smaha, O'Donnell, Bauers) declare a research collaboration with Niron Magnetics, Inc., a startup

company focused on commercializing $Fe_{16}N_2$, which may be perceived as a conflict of interest.

Open Access

References

1. US Department of Energy (DOE), *Quadrennial Technology Review 2015* (DOE, Washington, DC, 2015)
2. O. Gutfleisch, M.A. Willard, E. Brück, C.H. Chen, S.G. Sankar, J.P. Liu, *Adv. Mater.* **23**, 821 (2011). https://doi.org/10.1002/adma.201002180
3. US Department of Energy (DOE), *Critical Materials Assessment* (DOE, Washington, DC, 2023)
4. M. Sagawa, S. Fujimura, N. Togawa, H. Yamamoto, Y. Matsuura, *J. Appl. Phys.* **55**, 2083 (1984). https://doi.org/10.1063/1.333572
5. J.J. Croat, J.F. Herbst, R.W. Lee, F.E. Pinkerton, *J. Appl. Phys.* **55**, 2078 (1984). https://doi.org/10.1063/1.333571
6. S. Mugiraneza, A.M. Hallas, *Commun. Phys.* **5**, 95 (2022). https://doi.org/10.1038/s42005-022-00853-y
7. A. Trabesinger, *Nat. Phys.* **13**, 716 (2017). https://doi.org/10.1038/nphys4196
8. R.W. McCallum, L.H. Lewis, R. Skomski, M.J. Kramer, I.E. Anderson, *Annu. Rev. Mater. Res.* **44**, 451 (2014). https://doi.org/10.1146/annurev-matsci-070813-113457
9. J. Cui, J. Ormerod, D. Parker, R. Ott, A. Palasyuk, S. Mccall, M.P. Paranthaman, M.S. Kesler, M.A. McGuire, I.C. Nlebedim, C. Pan, T. Lograsso, *JOM* **74**, 1279 (2022). https://doi.org/10.1007/s11837-022-05156-9
10. J. Liu, G. Guo, X. Zhang, F. Zhang, B. Ma, J.-P. Wang, *Acta Mater.* **184**, 143 (2020). https://doi.org/10.1016/j.actamat.2019.11.052
11. E.A. Maslowski, *Electronically Commutated DC Motors for Electric Vehicles* (National Aeronautics and Space Administration, Lewis Research Center, 1981)
12. H. Kohlmann, T.C. Hansen, V. Nassif, *Inorg. Chem.* **57**, 1702 (2018). https://doi.org/10.1021/acs.inorgchem.7b02981
13. J.D. Rinehart, J.R. Long, *Chem. Sci.* **2**, 2078 (2011). https://doi.org/10.1039/C1SC00513H
14. P. Larson, I.I. Mazin, D.A. Papaconstantopoulos, *Phys. Rev. B* **67**, 214405 (2003). https://doi.org/10.1103/PhysRevB.67.214405
15. K. Kumar, *J. Appl. Phys.* **63**, R13 (1988). https://doi.org/10.1063/1.341084
16. M. Sagawa, S. Hirosawa, H. Yamamoto, S. Fujimura, Y. Matsuura, *Jpn. J. Appl. Phys.* **26**, 785 (1987)
17. B.-M. Ma, K. Narasimhan, J. Hurt, *IEEE Trans. Magn.* **22**, 1081 (1986). https://doi.org/10.1109/TMAG.1986.1064515
18. C. Abache, J. Oesterreicher, *J. Appl. Phys.* **60**, 3671 (1986). https://doi.org/10.1063/1.337574
19. W.B. Cui, Y.K. Takahashi, K. Hono, *Acta Mater.* **59**, 7768 (2011). https://doi.org/10.1016/j.actamat.2011.09.006
20. L. Liu, H. Sepehri-Amin, T. Ohkubo, M. Yano, A. Kato, T. Shoji, K. Hono, *J. Alloys Compd.* **666**, 432 (2016). https://doi.org/10.1016/j.jallcom.2015.12.227
21. J.M.D. Coey, *Engineering* **6**, 119 (2020). https://doi.org/10.1016/j.eng.2018.11.034
22. J. Cui, M. Kramer, L. Zhou, F. Liu, A. Gabay, G. Hadjipanayis, B. Balasubramanian, D. Sellmyer, *Acta Mater.* **158**, 118 (2018). https://doi.org/10.1016/j.actamat.2018.07.049
23. L. Zhou, M.K. Miller, P. Lu, L. Ke, R. Skomski, H. Dillon, Q. Xing, A. Palasyuk, M.R. McCartney, D.J. Smith, S. Constantinides, R.W. McCallum, I.E. Anderson, V. Antropov, M.J. Kramer, *Acta Mater.* **74**, 224 (2014). https://doi.org/10.1016/j.actamat.2014.04.044
24. K. Schnitzke, L. Schultz, J. Wecker, M. Katter, *Appl. Phys. Lett.* **57**, 2853 (1990). https://doi.org/10.1063/1.104202
25. L.H. Lewis, F.E. Pinkerton, N. Bordeaux, A. Mubarok, E. Poirier, J.I. Goldstein, R. Skomski, K. Barmak, *IEEE Magn. Lett.* **5**, 5500104 (2014). https://doi.org/10.1109/LMAG.2014.2312178
26. I.Z. Hlova, O. Dolotko, M. Abramchuk, A. Biswas, Y. Mudryk, V.K. Pecharsky, *J. Alloys Compd.* **981**, 173619 (2024). https://doi.org/10.1016/j.jallcom.2024.173619
27. J.R. Rumble (ed.), "Abundance of Elements in the Earth's Crust and in the Sea," in *CRC Handbook of Chemistry and Physics,* 104th edn. (Taylor & Francis, Internet Version, 2023) https://hbcp.chemnetbase.com/documents/01_05/01_05_0001.xhtml?dswid=1166. Accessed 21 Dec 2023
28. S.M. Fortier, N.T. Nassar, W.C. Day, J.M. Hammarstrom, R.R. Seal, G.E. Graham, G.W. Lederer, *Min. Eng.* **75**(5), 30 (2023)
29. H.-S. Li, J.M.D. Coey, "Magnetic Properties of Ternary Rare-Earth Transition-Metal Compounds," in *Handbook of Magnetic Materials,* vol. 6 (Elsevier, 1991), chap. 1, pp. 1–83. https://doi.org/10.1016/S1567-2719(05)80055-1
30. J.J.M. Franse, R.J. Radwański, "Magnet Properties of Binary Rare-Earth 3d-Transition-Metal Intermetallic Compounds," in *Handbook of Magnetic Materials,* vol. 7 (Elsevier, 1993), chap. 5, pp. 307–501. https://doi.org/10.1016/S1567-2719(05)80046-0
31. J.M.D. Coey, H. Sun, *J. Magn. Magn. Mater.* **87**, L251 (1990). https://doi.org/10.1016/0304-8853(90)90756-G
32. J.P. Liu, K. Bakker, F.R. de Boer, T.H. Jacobs, D.B. de Mooij, K.H.J. Buschow, *J. Less-Common Metals* **170**, 109 (1991). https://doi.org/10.1016/0022-5088(91)90056-A
33. J.M.D. Coey, H. Sun, D.P.F. Hurley, *J. Magn. Magn. Mater.* **101**, 310 (1991). https://doi.org/10.1016/0304-8853(91)90764-2
34. W. Xiang-Zhong, K. Donnelly, J.M.D. Coey, B. Chevalier, J. Etourneau, T. Berlureau, *J. Mater. Sci.* **23**, 329 (1988). https://doi.org/10.1007/BF01174072
35. X.-P. Zhong, R.J. Radwański, F.R. de Boer, T.H. Jacobs, K.H.J. Buschow, *J. Magn. Magn. Mater.* **86**, 333 (1990). https://doi.org/10.1016/0304-8853(90)90141-C
36. T. Iriyama, K. Kobayashi, N. Imaoka, T. Fukuda, H. Kato, Y. Nakagawa, *IEEE Trans. Magn.* **28**, 2326 (1992). https://doi.org/10.1109/20.179482
37. R. Kuchi, D. Schlagel, T.A. Seymour-Cozzini, J.V. Zaikina, I.Z. Hlova, *J. Alloys Compd.* **980**, 173532 (2024). https://doi.org/10.1016/j.jallcom.2024.173532
38. C.N. Christodoulou, T. Takeshita, *J. Alloys Compd.* **198**(1–2), 1 (1993). https://doi.org/10.1016/0925-8388(93)90137-C
39. N. Ji, X. Liu, J-P. Wang, *New J. Phys.* **12**, 063032 (2010). https://doi.org/10.1088/1367-2630/12/6/063032
40. Y. Jiang, M.A. Mehedi, E. Fu, Y. Wang, L.F. Allard, J.-P. Wang, *Sci. Rep.* **6**, 25436 (2016). https://doi.org/10.1038/srep25436
41. P.C.K. Vesborg, T.F. Jaramillo, *RSC Adv.* **2**, 7933 (2012). https://doi.org/10.1039/C2RA20839C
42. Niron Magnetics, "Niron Magnetics Secures $33M from Leading Automotive Manufacturers to Meet Growing Demand for Rare Earth-Free Magnets." https://www.nironmagnetics.com/news/niron-magnetics-secures-33m-from-leading-automotive-manufacturers-to-meet-growing-demand-for-rare-earth-free-magnets/. Press release, November 8, 2023. Accessed 22 Dec 2023
43. T.K. Kim, M. Takahashi, *Appl. Phys. Lett.* **20**, 492 (1972). https://doi.org/10.1063/1.1654030
44. X. Li, M. Yang, M. Jamali, F. Shi, S. Kang, Y. Jiang, X. Zhang, H. Li, S. Okatov, S. Faleev, A. Kalitsov, G. Yu, P.M. Voyles, O.N. Mryasov, J.-P. Wang, *Phys. Status Solidi Rapid Res. Lett.* **13**, 1900089 (2019). https://doi.org/10.1002/pssr.201900089.
45. X. Zhang, Y. Jiang, M. Yang, L.F. Allard, J.-P. Wang, *AIP Adv.* **6**, 056203 (2016). https://doi.org/10.1063/1.4943236
46. I. Opahle, H.K. Singh, J. Zemen, O. Gutfleisch, H. Zhang, *Phys. Rev. Res.* **2**, 023134 (2020). https://doi.org/10.1103/PhysRevResearch.2.023134
47. B. Balke, S. Wurmehl, G.H. Fecher, C. Felser, J. Kübler, *Sci. Technol. Adv. Mater.* **9**, 014102 (2008). https://doi.org/10.1088/1468-6996/9/1/014102
48. H. Hiraka, K. Ohoyama, Y. Ogata, T. Ogawa, R. Gallage, N. Kobayashi, M. Takahashi, B. Gillon, A. Gukasov, K. Yamada, *Phys. Rev. B* **90**, 134427 (2014). https://doi.org/10.1103/PhysRevB.90.134427
49. X. Hang, M. Matsuda, J.T. Held, K.A. Mkhoyan, J.-P. Wang, *Phys. Rev. B* **102**, 104402 (2020). https://doi.org/10.1103/PhysRevB.102.104402
50. S. Goto, H. Kura, E. Watanabe, Y. Hayashi, H. Yanagihara, Y. Shimada, M. Mizuguchi, K. Takanashi, E. Kita, *Sci. Rep.* **7**, 13216 (2017). https://doi.org/10.1038/s41598-017-13562-2
51. T. Kojima, M. Mizuguchi, T. Koganezawa, K. Osaka, M. Kotsugi, K. Takanashi, *Jpn. J. Appl. Phys.* **51**, 010204 (2012). https://doi.org/10.1143/JJAP.51.010204
52. E. Poirier, F.E. Pinkerton, R. Kubic, R.K. Mishra, N. Bordeaux, A. Mubarok, L.H. Lewis, J.I. Goldstein, R. Skomski, K. Barmak, *J. Appl. Phys.* **117**, 17E318 (2015). https://doi.org/10.1063/1.4916190
53. L.H. Lewis, P.S. Stamenov, *Adv. Sci.* (Weinheim) **11**(7), 2302696 (2024). https://doi.org/10.1002/advs.202302696
54. C.-W. Yang, D.B. Williams, J.I. Goldstein, *Geochim. Cosmochim. Acta* **61**, 2943 (1997). https://doi.org/10.1016/S0016-7037(97)00132-4

55. J. Paulevé, D. Dautreppe, J. Laugier, L. Néel, *J. Phys. Radium* **23**(10), 841 (1962). https://doi.org/10.1051/jphysrad:019620023010084100
56. L. Néel, J. Pauleve, R. Pauthenet, J. Laugier, D. Dautreppe, *J. Appl. Phys.* **35**, 873 (1964). https://doi.org/10.1063/1.1713516
57. L.H. Lewis, A. Mubarok, E. Poirier, N. Bordeaux, P. Manchanda, A. Kashyap, R. Skomski, J. Goldstein, F.E. Pinkerton, R.K. Mishra, R.C. Kubic Jr., K. Barmak, *J. Phys. Condens. Matter* **26**, 064213 (2014). https://doi.org/10.1088/0953-8984/26/6/064213
58. T. Keller, I. Baker, *Prog. Mater. Sci.* **124**, 100872 (2022). https://doi.org/10.1016/j.pmatsci.2021.100872
59. B. Balasubramanian, M. Sakurai, C.-Z. Wang, X. Xu, K.-M. Ho, J.R. Chelikowsky, D.J. Sellmyer, *Mol. Syst. Des. Eng.* **5**, 1098 (2020). https://doi.org/10.1039/D0ME00050G
60. B. Balamurugan, B. Das, W.Y. Zhang, R. Skomski, D.J. Sellmyer, *J. Phys. Condens. Matter* **26**, 064204 (2014). https://doi.org/10.1088/0953-8984/26/6/064204
61. M.K. Horton, J.H. Montoya, M. Liu, K.A. Persson, *NPJ Comput. Mater.* **5**, 64 (2019). https://doi.org/10.1038/s41524-019-0199-7
62. A. Vishina, O.Y. Vekilova, T. Björkman, A. Bergman, H.C. Herper, O. Eriksson, *Phys. Rev. B* **101**, 094407 (2020). https://doi.org/10.1103/PhysRevB.101.094407
63. Y. Iwasaki, R. Sawada, E. Saitoh, M. Ishida, *Commun. Mater.* **2**, 31 (2021). https://doi.org/10.1038/s43246-021-00135-0
64. H.K. Singh, Z. Zhang, I. Opahle, D. Ohmer, Y. Yao, H. Zhang, *Chem. Mater.* **30**, 6983 (2018). https://doi.org/10.1021/acs.chemmater.8b01618
65. G. Hautier, C. Fischer, V. Ehrlacher, A. Jain, G. Ceder, *Inorg. Chem.* **50**, 656 (2011). https://doi.org/10.1021/ic102031h
66. J.P.S. Walsh, S.M. Clarke, D. Puggioni, A.D. Tamerius, Y. Meng, J.M. Rondinelli, S.D. Jacobsen, D.E. Freedman, *Chem. Mater.* **31**, 3083 (2019). https://doi.org/10.1021/acs.chemmater.9b00385
67. P. Shankhari, O. Janka, R. Pöttgen, B.P.T. Fokwa, *J. Am. Chem. Soc.* **143**, 4205 (2021). https://doi.org/10.1021/jacs.0c10778
68. A. Jesche, R.W. McCallum, S. Thimmaiah, J.L. Jacobs, V. Taufour, A. Kreyssig, R.S. Houk, S.L. Budko, P.C. Canfield, *Nat. Commun.* **5**, 3333 (2014). https://doi.org/10.1038/ncomms4333
69. W.A. Merrill, T.A. Stich, M. Brynda, G.J. Yeagle, J.C. Fettinger, R. De Hont, W.M. Reiff, C.E. Schulz, R.D. Britt, P.P. Power, *J. Am. Chem. Soc.* **131**, 12693 (2009). https://doi.org/10.1021/ja903439t

Christopher L. Rom is a postdoctoral researcher in the Materials Science Center at the National Renewable Energy Laboratory. He received his PhD degree in materials chemistry from Colorado State University in 2022. His research focuses on solid-state synthesis of inorganic materials as bulk powders, aiming to make new materials for better magnets, batteries, and semiconductors. Rom can be reached by email at christopher.rom@nrel.gov.

Rebecca W. Smaha is a staff scientist in the Materials Science Center at the National Renewable Energy Laboratory (NREL). She received her PhD degree in chemistry from Stanford University in 2020 and was a Director's Postdoctoral Fellow at NREL from 2021 to 2023. Her research focuses on synthesizing and characterizing novel ternary nitrides as both bulk and film materials for potential applications as magnets, semiconductors, spintronics, and quantum materials. Smaha can be reached by email at rebecca.smaha@nrel.gov.

Shaun O'Donnell is a postdoctoral researcher in the Materials Science Center at the National Renewable Energy Laboratory. He received his PhD degree in solid-state chemistry from North Carolina State University in 2022. His research primarily focuses on the synthesis and characterization of transition-metal nitrides to develop structure–property relationships in nitride magnets. O'Donnell can be reached by email at shaun.odonnell@nrel.gov.

Sita Dugu is a postdoctoral researcher in the Materials Science Center at the National Renewable Energy Laboratory. She received her PhD degree in chemical physics from the University of Puerto Rico at Rio Piedras in 2021. Her research focuses on thin-film synthesis and characterization of novel ternary nitrides and phosphides to study structure, magnetic properties, and solar absorption. Dugu can be reached by email at sita.dugu@nrel.gov.

Sage R. Bauers is a staff scientist in the Materials Science Center at the National Renewable Energy Laboratory. He received his PhD degree in materials chemistry from the University of Oregon in 2016. His research is supported by the Office of Science at the US Department of Energy and broadly focuses on the experimental discovery and design of nascent energy materials. He currently leads programs on novel magnetic materials, topological semimetals, and alternative solar absorbers. Bauers can be reached by email at sage.bauers@nrel.gov.